Published in Photonics Technology Letters (IEEE) 8, issue 10, 1370 - 1372, 1996
which should be used for any reference to this work

A Monolithically Integrated Double Michelson Interferometer for Optical Displacement Measurement with Direction Determination

D. Hofstetter, H. P. Zappe, and R. Dändliker

Abstract— **A monolithically integrated optical displacement sensor fabricated in the GaAs–AlGaAs material system is reported. The single-chip device consists of a distributed Bragg reflector laser, two photodetectors, two phase modulators, two Y-couplers, and two directional couplers. It is configured as a double Michelson interferometer and allows the determination of both magnitude and direction of a displacement. The detection of two 90° phase-shifted interferometer signals also resulted in an improved phase interpolation of $\phi/20$. Despite the relatively simple fabrication process, the integration of rather complex optical functions could be realized.**

I. Introduction

INTEGRATED OPTICAL circuitry using III–V-semiconductors offers the possibility of monolithically integrating active and passive optical components. Such an integration is advantageous because of enhanced design flexibility, reduced or eliminated need for physical alignment procedures, greater robustness and potential for mass production.

Integrated optical displacement sensors have to date been fabricated on glass substrates using ion-exchanged strip waveguides by Jestel [1] and on silicon substrates with slab or ridge waveguides by Ulbers [2] and Voirin [3]. Two approaches employing III–V-semiconductor material, with the potential for integration as noted above, have been reported by Suhara [4] and by us [5]. Our previously reported device was single-Michelson-type, and, in contrast to the glass and silicon-based interferometers, not able to detect the direction of the movement. To the best of our knowledge, no III–V-based device allowing the measurement of two independent phase-shifted interference signals with an integrated laser has yet been published.

In this work, we describe a double Michelson interferometer consisting of one DBR laser, two photodetectors, two phase modulators, two Y-couplers, and two directional couplers with which both magnitude and direction of a movable external object could be measured. As can be seen in the schematic of Fig. 1, the light of the DBR laser was divided into two nearly independent Michelson interferometers by a Y-coupler. A relative phase shift between the two reference arms was generated by phase modulators allowing the detection of two interference signals in phase quadrature and thus the changes in displacement direction. Interference signals could be measured at mirror distances of up to 20 cm with sub-100-nm resolution.

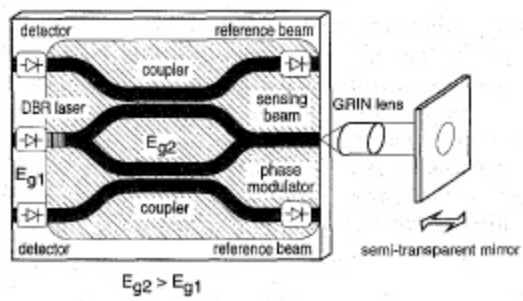

Fig. 1. Schematic of the monolithically integrated double Michelson displacement sensor with direction determination. The diode symbols in the reference beams represent the phase modulators.

This displacement measurement chip was fabricated on a double heterostructure layer sequence requiring only a single growth step. A vacancy-enhanced disordering (VED) process was employed to define absorbing photodetector and pumped laser areas as well as transparent waveguiding sections [6]. In addition, a simplified DBR laser process using a grating recess allowed the integration of all necessary optical functions with a relatively simple technology.

II. Technology

The layer structure used for these devices was grown by metal-organic vapor phase epitaxy on a GaAs substrate (n-doped 10^{18} cm^{-3} Si) and included an undoped 165-nm-thick $Al_{0.3}Ga_{0.7}As$ waveguide core containing a single GaAs quantum well (7 nm). This layer was sandwiched between a 1.1-μm-thick $Al_{0.8}Ga_{0.2}As$ lower cladding layer (n-doped 1.5×10^{18} cm^{-3} Si) and an 0.85-μm-thick $Al_{0.8}Ga_{0.2}As$ upper cladding layer (p-doped 10^{18} cm^{-3} Mg). A 160-nm-thick highly p-doped (5×10^{18} cm^{-3} Zn) GaAs cap layer completed the structure.

Integration of lasers, photodetectors, modulators and waveguides requires compatible process technologies for all necessary components of the circuit. For this work, we employed processes reported previously, namely the fabrication of a single growth step DBR laser [7], [8] and the selective, partial

D. Hofstetter and H. P. Zappe are with the Paul Scherrer Institute, Badenerstrasse 569, 8048 Zurich, Switzerland.
R. Dändliker is with the Institute of Microtechnology, University of Neuchâtel, Rue A.-L. Breguet 2, 2000 Neuchâtel, Switzerland.

intermixing of quantum wells for postgrowth bandgap-shifting [9]. Proton implantation (H^+, 4×10^{15} cm^{-2}, 40/70/100 keV) was used to generate a high electrical resistance between laser and photodetectors (>10 GΩ), and the reduction of optical crosstalk between these two elements was achieved by dry etching an isolation trench. This trench was filled with the p-metallization layers to prevent the light from going directly from the laser into the photodetector.

III. Interferometer Description

The optical circuits described in this letter were configured as double Michelson interferometers, shown schematically in Fig. 1. The ridge width of the waveguides was 3 μm and the curve radii were 500 μm. All passive waveguides were fabricated in the areas with intermixed quantum wells and had an absorption loss of 35–45 dB/cm, due to the relatively small bandgap difference of 45 meV between intermixed *(bandgap energy E_{g2})* and nonintermixed *(bandgap energy E_{g1})* sections. Since the total waveguide length did not exceed 3 mm, this relatively high absorption loss was not overly detrimental for interferometer performance.

For the splitting of the incoming light into the reference and sensing arms, we used either directional couplers with a length of 500 μm or, in an alternative design, Y-couplers. Depending on the type of coupler used, the total cleaved chip length was 1.95 mm for devices with Y-couplers or 2.6 mm for those with directional couplers. Modulator length was 340 μm; when driven at -12-V reverse voltage, we measured a one-pass phase shift of $\pi/16$.

Both the pumped laser section and photodetectors were fabricated in the nonintermixed, and thus absorbing, areas of the chip and had a length of 500 μm each. The length of the nonabsorbing DBR grating section was 200 μm; we used a third-order grating with a period of 380 nm, a depth of 150 nm and a 1:1 line-to-space ratio. A 70-nm thin buffer layer between the bottom of the grating and the waveguide core resulted in a calculated grating coupling coefficient of 100 cm^{-1}; this gave the desired grating reflection coefficient of about 95%. The left cleaved facet of the interferometer served as second laser mirror.

The DBR lasers of our displacement sensors were driven CW at room temperature. Typical threshold currents were 30 mA, corresponding to a threshold current density of 2 kA/cm^2. The emission wavelength was 822 nm and the spectrum showed a sidemode suppression ratio of approximately 25–30 dB. For interferometric measurements, the lasers were usually operated at 50 mA. At this current level, 2 mW of optical power was emitted from the left cleaved facet of the device. A measurement of the output power from the grating side was performed indirectly by coupling its light through a straight waveguide into a photodetector. Under the assumption of 40 dB/cm waveguide loss, we estimated the output power into the interferometer to be around 2 μW. This asymmetry of the optical output power was due to the different reflectances (facet: 30%, grating: 95%) of the two laser mirrors.

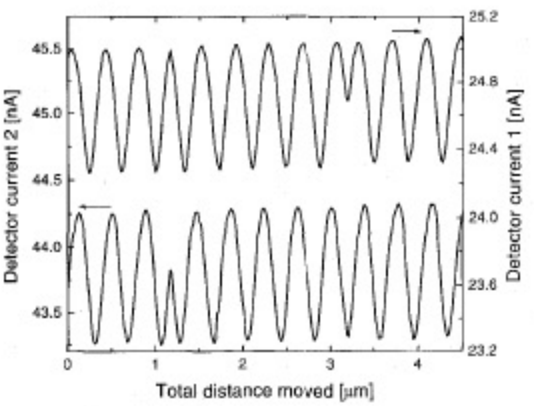

Fig. 2. The two detector currents $I(\phi)$ of the double Michelson interferometer for 3.5 cm *mirror* distance and 67% *mirror* reflectance showing the two interference signals. Direction changes occurred at 1.2 μm and at 3.2 μm.

IV. Performance

The measurement setup for interferometer characterization consisted of a Peltier temperature-stabilized mount for the interferometer bars, an external, independently movable GRIN lens (pitch = 0.23) for measurement beam collimation and a piezo-driven, semitransparent mirror as measurement object (67% reflectance). A CCD camera-based imaging system allowed rough alignment of the measurement beam into auto-collimation. Fine adjustment was performed by optimizing the detector signals during the measurement. The travel of the displacement piezoactuator was restricted to 20 μm; the movement was stimulated by a symmetric sawtooth voltage signal from a function generator. The amplitude of the voltage was adjusted to change the direction of the movement after every 2 μm of displacement.

Fig. 2 shows the result of an interferometric measurement at a mirror distance of 3.5 cm. The dc components of the interferometer signal, defined by

$$I(\phi) = I_{\text{cross}} + \frac{I_0}{2}(1 + V \cdot \cos\phi)$$

include a constant offset in the detector current signal, I_{cross}, due to optical crosstalk between laser and detector, as well as the component $I_0/2$ due to visibility, $V = (I_{\max} - I_{\min})/(I_{\max} + I_{\min})$, less than unity. In Fig. 2, there are two changes of the movement direction: one at 1.2 μm and another at 3.2 μm. One interference fringe corresponds to a mirror movement of one half of the measurement wavelength, namely 411 nm. The amplitudes of the detector current signals, $(I_0 V/2)$, were 0.5 nA and 0.4 nA. Optical crosstalk signals of 35 nA and 16 nA, respectively, were seen because of the insufficiently deep isolation trench. The value of the crosstalk could be accurately determined by measuring the latter in an uncleaved interferometer bar; this approach suppressed all reflections at the measurement facet.

Plotting the two interferometer detector currents, $I(\phi)$, against each other resulted in a Lissajous-figure as shown in Fig. 3. The ratio of the two normalized ellipse main-axes allowed an estimate of the phase shift between the two signals, approximately 75°–80°. With a longer phase modulator, it

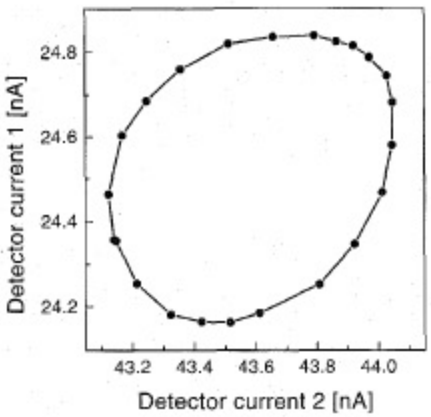

Fig. 3. Lissajous-figure of the two detector currents for 3.5-cm mirror distance and 67% mirror reflectance. Resolution of the measurement is about $\Delta\phi_{\min} = \phi/20$.

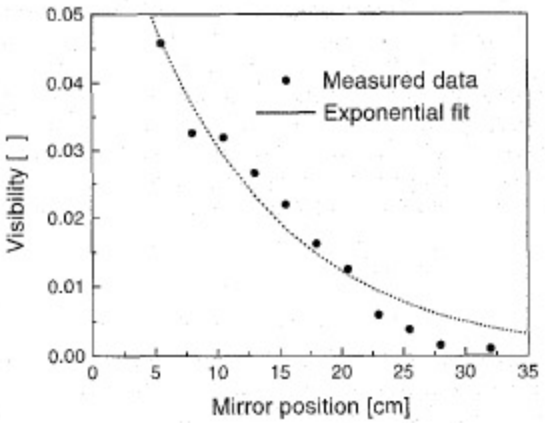

Fig. 4. Signal visibility versus mirror distance of a simple Michelson interferometer of the same fabrication run. This result implies a laser linewidth of $\Delta\nu = 800$ MHz.

should be possible to adjust the phase shift to the desired value of 90°. Nevertheless, a phase interpolation of $\phi/20$, resulting in 20-nm resolution of the displacement measurement, should be possible.

The slightly distorted sine- and cosine-shape of the two signals results from the parasitic reflection at the right cleaved facet of the sensing beam. This reflection at the measurement facet and the reflection at the object mirror generate a Fabry–Pérot interferometer cavity, whose optical field interferes with the one from the reference arm. We studied the behavior of such a three-mirror interferometer by simulation and were able to predict the experimentally measured asymmetric shape of the interferograms when changing the intrinsic phase between reference and sensing arm.

Fig. 4 shows the interference signal visibility, V, as a function of mirror distance for a single Michelson interferometer. A Fourier-transformation of this so-called autocorrelation function allowed a determination of the laser linewidth. Although typical DBR lasers, with a linewidth of 1 MHz or less, have coherence lengths of several hundred meters, the rapid decay of visibility with increasing distance as seen in the figure results from an enhanced linewidth of about 800 MHz. This increase is probably caused by the perturbation of the DBR laser through feedback from the cleaved right facet. In addition, the modal behavior of the sensing beam waveguide was not ideal; we could occasionally observe higher order waveguide modes under different coupling conditions. This effect also reduced the visibility and gave raise to "mode hopping" in the feedback, which was clearly indicated by spontaneous changes of the phase between the two interferometer signals.

V. Conclusion/Outlook

A monolithically integrated double Michelson interferometer for displacement measurement with direction determination was designed, fabricated and characterized. The device consisted of a DBR laser, detectors, modulators and waveguides, all fabricated on a single GaAs–AlGaAs-chip. Displacement measurements were performed using only one external element for beam collimation and a movable mirror as measurement object. Although using relatively simple standard processing technologies, we could demonstrate the fabrication of an advanced monolithic device with complex optical functions.

Acknowledgment

The authors are grateful to J. E. Epler and H. P. Schweizer for crystal growth; P. Riel, D. Jeggle and A. Vonlanthen for processing assistance; and J. Söchtig, M. T. Gale, and H. W. Lehmann for their generous support.

References

[1] D. Jestel, A. Baus and E. Voges, "Integrated-optic interferometric microdisplacement sensor in glass with thermo-optic phase modulation," *Electron. Lett.*, vol. 26, no. 15, pp. 1144–1145, 1990.

[2] G. Ulbers, "An integrated optics sensor on silicon for the measurement of displacement, force and refractive index," *Proc. SPIE, Micro-Optics II*, vol. 1506, 1991, pp. 99–110.

[3] G. Voirin, L. Falco, O. Boillat, O. Zogmal, P. Regnault, and O. Parriaux, "Monolithic double interferometer displacement sensor with wavelength stabilization," *Proc. Eur. Conf. Integrat. Opt. 93*, 1993, pp. 12-28–12-29.

[4] T. Suhara, T. Taniguchi, M. Uemukai. H. Nishihara, T. Hirata, S. Iio, and M. Suehiro, "Monolithic integrated-optic position/displacement sensor using waveguide ratings and QW-DFB laser," *IEEE Photon. Technol. Lett.*, vol. 7, no. 10, pp. 1195–1197, 1995.

[5] D. Hofstetter, H. P. Zappe, and R. Dändliker, "Monolithically integrated optical displacement sensor in GaAs/AlGaAs," *Electron. Lett.*, vol. 31, no. 24, pp. 2121–2122, 1995.

[6] J. Beauvais, J. H. Marsh, A. H. Kean, A. C. Bryce, and C. Button, "Suppression of bandgap shifts in GaAs/AlGaAs quantum wells using strontium fluoride caps," *Electron. Lett.*, vol. 28, pp. 1670–1672, 1992.

[7] D. Hofstetter, H. P. Zappe, J. E. Epler and J. Söchtig, "Single-growth-step GaAs/AlGaAs distributed Bragg reflector lasers with holographically-defined recessed gratings", *Electron. Lett.*, vol. 30, pp. 1858–1859, 1994.

[8] D. Hofstetter, H. P. Zappe, and J. E. Epler, "Ridge waveguide DBR lasers with nonabsorbing grating and transparent integrated waveguide," *Electron. Lett.*, vol. 31, no. 12, pp. 980–982, 1995.

[9] D. Hofstetter, H. P. Zappe, J. E. Epler, and P. Riel, "Multiple wavelength Fabry-Pérot lasers fabricated by vacancy-enhanced quantum well disordering," *Appl. Phys. Lett.*, vol. 67, pp. 1978–1980, 1995.